Polarization selective beam shaping using nanoscale dielectric metasurfaces

Boris Desiatov,[1] Noa Mazurski,[1] Yeshaiahu Fainman[2] and Uriel Levy[1,*]

[1]*Department of Applied Physics, The Benin School of Engineering and Computer Science, The Center for Nanoscience and Nanotechnology, The Hebrew University of Jerusalem, Jerusalem, 91904, Israel*
[2]*Department of Electrical and Computer Engineering, University of California, San Diego, 9500 Gilman Drive, La Jolla, CA 92093-0407,USA*
[*]ulevy@mail.huji.ac.il

Abstract: Metasurfaces consisting of ultrathin nanostructures are utilized to control the properties of light including its phase, amplitude and polarization. Hereby, we demonstrate the capability of such structures to perform arbitrary polarization selective beam shaping using dielectric nanoscale metasurfaces implemented in silicon. By illuminating the structure with right handed circular polarization we reconstruct a desired image. When switching the polarization into its orthogonal state, we obtain the reconstruction of a different image. This demonstration shows the potential of using dielectric metasurfaces for high efficiency beam shaping applications in general, and specifically for polarization coded beam shaping.

©2015 Optical Society of America

OCIS codes: (230.5440) Polarization-selective devices; (160.3918) Metamaterials.

References and links

1. M. Born and E. Wolf, *Principles of Optics: Electromagnetic Theory of Propagation, Interference and Diffraction of Light*, 7th ed. (Cambridge University Press, 1999).
2. A. G. Lopez and H. G. Craighead, "Wave-plate polarizing beam splitter based on a form-birefringent multilayer grating," Opt. Lett. **23**(20), 1627–1629 (1998).
3. P. Lalanne, J. Hazart, P. Chavel, E. Cambril, and H. Launois, "A transmission polarizing beam splitter grating," J. Opt. A, Pure Appl. Opt. **1**(2), 215–219 (1999).
4. F. Xu, R. C. Tyan, P. C. Sun, Y. Fainman, C. C. Cheng, and A. Scherer, "Fabrication, modeling, and characterization of form-birefringent nanostructures," Opt. Lett. **20**(24), 2457–2459 (1995).
5. I. Richter, P.-C. Sun, F. Xu, and Y. Fainman, "Design considerations of form birefringent microstructures," Appl. Opt. **34**(14), 2421–2429 (1995).
6. Z. Bomzon, G. Biener, V. Kleiner, and E. Hasman, "Space-variant Pancharatnam-Berry phase optical elements with computer-generated subwavelength gratings," Opt. Lett. **27**(13), 1141–1143 (2002).
7. N. Passilly, K. Ventola, P. Karvinen, P. Laakkonen, J. Turunen, and J. Tervo, "Polarization conversion in conical diffraction by metallic and dielectric subwavelength gratings," Appl. Opt. **46**(20), 4258–4265 (2007).
8. C. Gu and P. Yeh, "Form birefringence dispersion in periodic layered media," Opt. Lett. **21**(7), 504–506 (1996).
9. J. Tervo, V. Kettunen, M. Honkanen, and J. Turunen, "Design of space-variant diffractive polarization elements," J. Opt. Soc. Am. A **20**(2), 282–289 (2003).
10. U. Levy, C.-H. Tsai, L. Pang, and Y. Fainman, "Engineering space-variant inhomogeneous media for polarization control," Opt. Lett. **29**(15), 1718–1720 (2004).
11. U. Levy, H.-C. Kim, C.-H. Tsai, and Y. Fainman, "Near-infrared demonstration of computer-generated holograms implemented by using subwavelength gratings with space-variant orientation," Opt. Lett. **30**(16), 2089–2091 (2005).
12. T. Kaempfe, P. Sixt, D. Renaud, A. Lagrange, F. Perrin, and O. Parriaux, "Linear to radial/azimuthal polarization converter in transmission using form birefringence in a segmented silicon grating manufactured by high productivity microelectronic technologies," in (2014), Vol. 9130, p. 91300W–91300W–7.
13. Z. Bomzon, G. Biener, V. Kleiner, and E. Hasman, "Radially and azimuthally polarized beams generated by space-variant dielectric subwavelength gratings," Opt. Lett. **27**(5), 285–287 (2002).
14. G. M. Lerman and U. Levy, "Generation of a radially polarized light beam using space-variant subwavelength gratings at 1064 nm," Opt. Lett. **33**(23), 2782–2784 (2008).
15. W. S. Mohammed, A. Mehta, M. Pitchumani, and E. G. Johnson, "Selective excitation of the TE_{01} mode in hollow-glass waveguide using a subwavelength grating," Photonics Technol. Lett. IEEE **17**(7), 1441–1443 (2005).
16. N. Yu and F. Capasso, "Flat optics with designer metasurfaces," Nat. Mater. **13**(2), 139–150 (2014).

17. A. V. Kildishev, A. Boltasseva, and V. M. Shalaev, "Planar Photonics with Metasurfaces," Science **339**(6125), 1232009 (2013).
18. A. Pors, M. G. Nielsen, R. L. Eriksen, and S. I. Bozhevolnyi, "Broadband Focusing Flat Mirrors Based on Plasmonic Gradient Metasurfaces," Nano Lett. **13**(2), 829–834 (2013).
19. M. Decker, I. Staude, M. Falkner, J. Dominguez, D. N. Neshev, I. Brener, T. Pertsch, and Y. S. Kivshar, "High-Efficiency Dielectric Huygens' Surfaces," Adv. Opt. Mater. **3**(6), 813–820 (2015).
20. P. Moitra, B. A. Slovick, Z. G. Yu, S. Krishnamurthy, and J. Valentine, "Experimental demonstration of a broadband all-dielectric metamaterial perfect reflector," Appl. Phys. Lett. **104**(17), 171102 (2014).
21. D. Lin, P. Fan, E. Hasman, and M. L. Brongersma, "Dielectric gradient metasurface optical elements," Science **345**(6194), 298–302 (2014).
22. Y. F. Yu, A. Y. Zhu, R. Paniagua-Domínguez, Y. H. Fu, B. Luk'yanchuk, and A. I. Kuznetsov, "High-transmission dielectric metasurface with 2π phase control at visible wavelengths," Laser Photonics Rev. **9**(4), 412–418 (2015).
23. A. Arbabi, Y. Horie, M. Bagheri, and A. Faraon, "Complete control of polarization and phase of light with high efficiency and sub-wavelength spatial resolution," arXiv:1411.1494v1 [physics.optics] (2014).
24. A. Arbabi, Y. Horie, A. J. Ball, M. Bagheri, and A. Faraon, "Subwavelength-thick lenses with high numerical apertures and large efficiency based on high-contrast transmitarrays," Nat. Commun. **6**, 7069 (2015).
25. R. Paniagua-Dominguez, Y. F. Yu, A. E. Miroschnichenko, L. A. Krivitsky, Y. H. Fu, V. Valuckas, L. Gonzaga, Y. T. Toh, A. Y. S. Kay, B. Luk'yanchuk, and A. I. Kuznetsov, "Generalized Brewster-Kerker effect in dielectric metasurfaces," 12 (2015).
26. S. Liu, M. B. Sinclair, T. S. Mahony, Y. C. Jun, S. Campione, J. Ginn, D. A. Bender, J. R. Wendt, J. F. Ihlefeld, P. G. Clem, J. B. Wright, and I. Brener, "Optical magnetic mirrors without metals," Optica **1**(4), 250 (2014).
27. K. E. Chong, I. Staude, A. James, J. Dominguez, S. Liu, S. Campione, G. S. Subramania, T. S. Luk, M. Decker, D. N. Neshev, I. Brener, and Y. S. Kivshar, "Polarization-independent silicon metadevices for efficient optical wavefront control," Nano Lett. **15**(8), 5369–5374 (2015).
28. Y. H. Fu, A. I. Kuznetsov, A. E. Miroshnichenko, Y. F. Yu, and B. Luk'yanchuk, "Directional visible light scattering by silicon nanoparticles," Nat. Commun. **4**, 1527 (2013).
29. Y. Yang, W. Wang, P. Moitra, I. I. Kravchenko, D. P. Briggs, and J. Valentine, "Dielectric Meta-Reflectarray for Broadband Linear Polarization Conversion and Optical Vortex Generation," Nano Lett. **14**(3), 1394–1399 (2014).
30. N. Yu, P. Genevet, M. A. Kats, F. Aieta, J.-P. Tetienne, F. Capasso, and Z. Gaburro, "Light Propagation with Phase Discontinuities: Generalized Laws of Reflection and Refraction," Science **334**(6054), 333–337 (2011).
31. W. T. Chen, K.-Y. Yang, C.-M. Wang, Y.-W. Huang, G. Sun, I.-D. Chiang, C. Y. Liao, W.-L. Hsu, H. T. Lin, S. Sun, L. Zhou, A. Q. Liu, and D. P. Tsai, "High-Efficiency Broadband Meta-Hologram with Polarization-Controlled Dual Images," Nano Lett. **14**(1), 225–230 (2014).
32. C. Pfeiffer, C. Zhang, V. Ray, L. J. Guo, and A. Grbic, "High performance bianisotropic metasurfaces: asymmetric transmission of light," Phys. Rev. Lett. **113**(2), 023902 (2014).
33. E. Hasman, V. Kleiner, G. Biener, and A. Niv, "Polarization dependent focusing lens by use of quantized Pancharatnam–Berry phase diffractive optics," Appl. Phys. Lett. **82**(3), 328–330 (2003).
34. I. Moreno, J. A. Davis, T. M. Hernandez, D. M. Cottrell, and D. Sand, "Complete polarization control of light from a liquid crystal spatial light modulator," Opt. Express **20**(1), 364–376 (2012).
35. R.-C. Tyan, P. C. Sun, and Y. Fainman, "Polarizing beam splitters constructed of form-birefringent multilayer gratings," In **2689**, 82–89 (1996).
36. B. Walther, C. Helgert, C. Rockstuhl, F. Setzpfandt, F. Eilenberger, E.-B. Kley, F. Lederer, A. Tünnermann, and T. Pertsch, "Spatial and spectral light shaping with metamaterials," Adv. Mater. **24**(47), 6300–6304 (2012).
37. R. Gerchberg and W. Saxton, "A practical algorithm for the determination of phase from image and diffraction plane pictures," Optik **35**, 237–250 (1971).

1. Introduction

Controlling the refractive index of materials at will is a prime goal of photonics research. It is well known that the refractive index can be manipulated by structuring the material at the subwavelength scale [1], using the concept of effective index. Over the years, this capability had led to a large number of demonstrations in which artificial dielectric materials has been created [2–11]. In particular, such structures exhibit strong birefringence properties, also known as "form birefringence", which can be an order of magnitude higher than the birefringence of natural materials. Using this property, numerous demonstrations of polarization transformations could be achieved, including for example the generation of radially and azimuthally polarized light [12–15]. Following this plethora of demonstrations, recent years brought into the forefront the concept of metallic metasurface, in which thin metallic nanostructures have been used for the purpose of controlling the properties of light [16–18] polarization of the incident beam, yet with limited energetic efficiency due to the ohmic loss in the metal. The latter claim is particularly true for transmission type devices. This limitation has tailored the research focus back towards dielectric metasurfaces, with

several recent important demonstrations, e.g. the use of thin silicon nanoantennas for phase and polarization control [19–27] as well as directional light scattering and reflection [28,29].

Hereby, we demonstrate the capability of a dielectric metasurface to perform arbitrary polarization selective beam shaping. While polarization selectivity in such structures has been observed, e.g. for the purpose of polarization and wavelength dependent focusing and splitting [30–36], achieving an arbitrary polarization selective beam shaping with a single dielectric metasurface is yet to be demonstrated. Specifically, we show here for the first time that by modifying the polarization of an incident beam of light one can switch between two arbitrarily chosen images. It should be noticed that polarization selective hologram was recently demonstrated in metallic metasurfaces in reflection configuration [32].

2. Theoretical background

We begin by defining the problem in hand. Given a single metasurface, we would like to illuminate it by a right handed circularly polarized light and achieve a reconstruction of a desired image at a specific distance away of the metasurface. Furthermore, by switching the polarization to its left handed orthogonal state, the same metasurface should provide a reconstruction of a different image per our choice, which is located at the same image plane. This is shown schematically in Fig. 1.
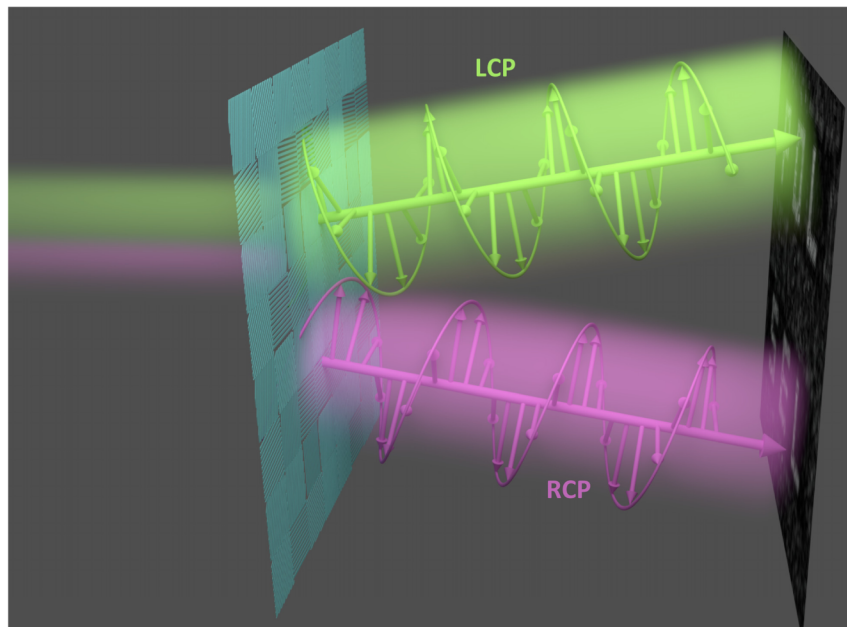

Fig. 1. Schematic representation of our structure.

We now turn into selecting our metasurface and study its properties. Our metasurface consists of a pixilated structure. In each pixel, a subwavelength periodic structure is defined and etched into the silicon substrate. A schematic representation of this structure is given in Fig. 2.
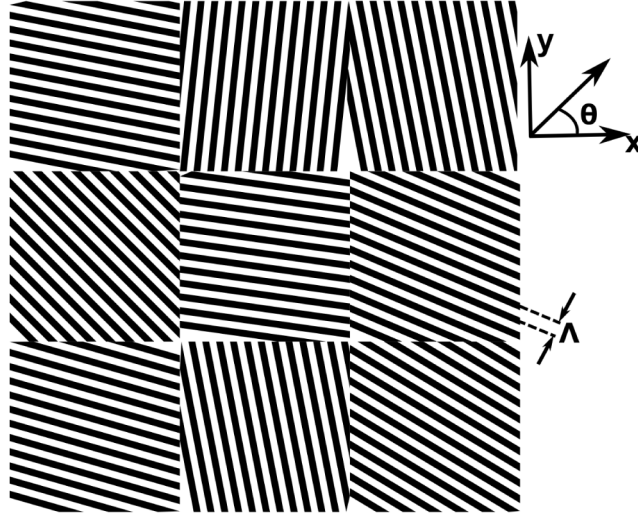
Fig. 2. Schematic representation showing a top view of our dielectric metasurface. In each pixel a nanoscale subwavelength 1-D grating is defined. The orientation of this structure is kept as a free parameter and is used to control the phase of the light emanating from our metasurface.

We consider a plane wave transmitted through the metasurface located at $z = 0$, with x and y being the transverse coordinates. Neglecting Fresnel reflections, the transmitted field is given by,

$$ET(x, y, z = 0^+) = \overline{\overline{R}}(x, y)^{-1}\overline{\overline{G}}\overline{\overline{R}}(x, y)V_{in} \tag{1}$$

Where

$$\overline{\overline{R}}(x, y) = \begin{bmatrix} \cos[\theta(x, y)] & \sin[\theta(x, y)] \\ -\sin[\theta(x, y)] & \cos[\theta(x, y)] \end{bmatrix} \text{ and } \overline{\overline{G}}(x, y) = \begin{bmatrix} \exp(-i\phi(x, y)/2) & 0 \\ 0 & \exp(i\phi(x, y)/2) \end{bmatrix}$$

are the rotation and the Jones matrix, respectively, and V_{in} represents the Jones vector of the incident field. The matrix G describes the birefringence of the subwavelength grating in each pixel. The obtained phase retardation, $\phi(x,y)$ is determined by the geometry of the subwavelength grating (duty cycle and grating depth), and by the refractive index of the substrate material. $\theta(x,y)$ represents the orientation angle of the subwavelength grating at each pixel with respect to the x axis (see Fig. 2). The validity of Eq. (1) relies on the thin element approximation, which holds as long as the pixel size is large and the grating depth is not too large compared to the wavelength. Assuming constant retardation for each of the pixels (i.e. the grating is identical at each pixel, with the result of space invariant values of ϕ and G), the rotation angle $\theta(x, y)$ is the only free parameter.

For right and left hand circularly polarized (RCP and LCP respectively) incident light with the corresponding Jones vectors $V_{inR} = [1, i]^T$ and $V_{inL} = [1, -i]^T$, we can now express Eq. (1) as [6,10,11],

$$E_{TR}(x, y, z = 0^+) = \cos(\phi/2)\begin{bmatrix} 1 \\ i \end{bmatrix} - i\sin(\phi/2)\exp[+i2\theta(x, y)]\begin{bmatrix} 1 \\ -i \end{bmatrix} \tag{2a}$$

and

$$E_{TL}\left(x,y,z=0^{+}\right)=\cos\left(\phi/2\right)\begin{bmatrix}1\\-i\end{bmatrix}-i\sin\left(\phi/2\right)\exp\left[-i2\theta\left(x,y\right)\right]\begin{bmatrix}1\\i\end{bmatrix} \quad (2b)$$

respectively.

The cosine term can be eliminated by designing the grating parameters such that a π phase retardation ($\phi = \pi$) is achieved. For such a case, the metasurface provides pure phase modulation, with the obtained phase being twice the rotation angle. Therefore, the desired phase modulation can be achieved simply by varying the orientation of the periodic structure in each pixel, such that a continuous phase modulation is achieved using a binary grating. This approach eliminates the need for complicated multiple step or gray scale fabrication procedures, significantly reducing the fabrication complexity and cost. We used pixel size of 8 micron to be larger then the wavelength of optical fields to allow validity of thin element approximation [37]. The pixel size can be further decreased down to about 3 microns [11] while preserving the good performance of the hologram. The 8 micron pixel size was chosen as a convenient number which is comparable to commercial available liquid crystal on silicon spatial light modulators. Further reduction of the pixel size is possible, nut requires a slightly different mechanism, in which the scattering efficiency from a single rod is enhanced by operating close to resonance.

3. Design and simulations

Our device was designed based on a modified version of the Gerchberg Saxton (G-S) algorithm [37]. Specifically, we take advantage of the phase degree of freedom, namely, we are only interested in the amplitude of the reconstructed images, and thus their phases can be used as free parameters.

Our goal is to achieve two independent images in the Fresnel domain, at a distance Z0 away of the metasurface plane. If illuminated by RCP the complex transmission function of the metasurface is given by H(x,y), while for LCP illumination, the complex transmission function of the metasurface is given by -H*(x,y). In the output plane, the images are given by the Fresnel transform, i.e.

$$f_1\left(x",y"\right)=FSP\left(H\left(x,y\right),Z_0\right)=\frac{\exp\left(ikZ_0\right)}{i\lambda Z_0}\exp\left(i\frac{k}{2Z_0}\left(x"^2+y"^2\right)\right)$$
$$\int_{-\infty}^{\infty}\int_{-\infty}^{\infty}H\left(x,y\right)\exp\left(i\frac{k}{2Z_0}\left(x^2+y^2\right)\right)\exp\left(-i\frac{2\pi}{\lambda Z_0}\left(xx"+yy"\right)\right)dxdy \quad (3a)$$

and:

$$f_2\left(x",y"\right)=FSP\left(-H^{*}\left(x,y\right),Z_0\right)=-\frac{\exp\left(ikZ_0\right)}{i\lambda Z_0}\exp\left(i\frac{k}{2Z_0}\left(x"^2+y"^2\right)\right)$$
$$\int_{-\infty}^{\infty}\int_{-\infty}^{\infty}H\left(x,y\right)\exp\left(i\frac{k}{2Z_0}\left(x^2+y^2\right)\right)\exp\left(-i\frac{2\pi}{\lambda Z_0}\left(xx"+yy"\right)\right)dxdy \quad (3b)$$

Can the two distributions $f_1\left(x",y"\right)$ and $f_2\left(x",y"\right)$ represent two non-identical intensity functions? Indeed, this is possible. We now release all restrictions on the displayed phase, and only require that the amplitude of those distributions should match the desired to images.

We now need to find the function H(x,y) which can generate the desired distributions I_1 and I_2. Such a function can be found by using the G-S algorithm, bearing in mind that the amplitude distribution of f_1 and f_2 are the constraints i.e. $\left|f_1\right|^2=I_1, \left|f_2\right|^2=I_2$. While the phase distributions are free parameters with no restrictions. Applying the G-S algorithm with these

constraints, we can find the function H(x,y) that would reconstruct the two desired images with minimal error.

4. Fabrication and measurements

After calculating the value of H(x,y) we can now turn into fabricating the actual device which will produce the desired phase distribution. First, we find the desired rotation angle for each pixel which is simply half of the phase of H(x,y). Once the orientation of the grating is know, we have all the needed parameters for the device fabrication. Our metasurface was fabricated on a double sided polished 2-inch p-type silicon wafer. First, an etching mask was defined in the resist (ZEP 520A) by Electron Beam Lithography (Raith E_Line 150). Next the pattern was transferred to the silicon substrate by Reactive Ion Etching (Corial 200RL) of silicon (depth ~500nm to provide π retardation). Finally the resist was stripped and the fabricated element was inspected in Scanning Electron Microscope (SEM), and a top view of the final structure is shown in a Fig. 3. The metasurface consist of 128X128 pixels, 8 micron each with sub wavelength grating ($\Lambda = 400nm$, duty cycle 50%) embedded into each pixel.
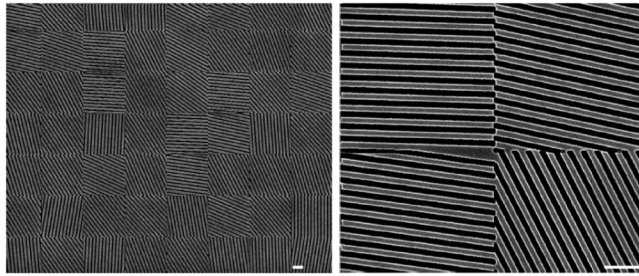

Fig. 3. Left - Scanning Electron Microscope micrographs showing a top view of fabricated device. Right - Magnified image. Scale bar is 2 micron in both figures.

To characterized the polarization selective dielectric metasurface we illuminated the device at a wavelength of 1550 nanometer using a single lens imaging system (F = 150mm) with a magnification of 4. A fiber coupled laser (Thorlabs S3FC1550) was connected to the laser collimator followed by a quarter wave plate that was mounted on a manual rotation stage for converting the incident linearly polarized beam into left and right circularly polarized beam. A near-infrared InGaAs 2-D focal plane array (Sensors Unlimited) was placed at some distance away of the back focal plane of the optical system in order to capture the images in the Fresnel domain. The schematic diagram of measurement system is shown in Fig. 4.
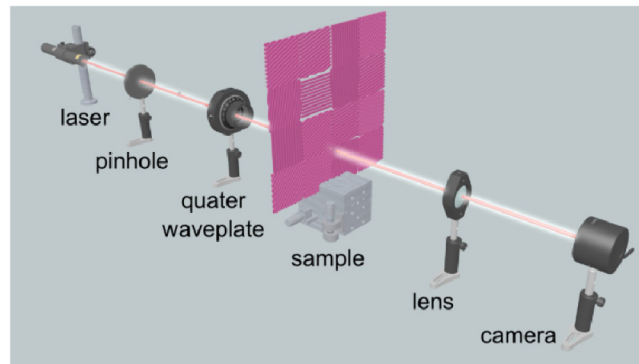

Fig. 4. Schematic diagram of the experimental setup.

The obtained experimental results for RCP and LCP incident beams are shown in Fig. 5 a,b respectively. The corresponding computer simulation results with the same color scheme as the obtained results are presented in Fig. 5 c,d respectively. As an example, the two set of

letter "POL" and "SEL" were selected, to represent the polarization selective property of our dielectric metasurface. The calculated purity of the reconstructed image in the simulation, defined as a ratio between the all optical power of the image and the integrated optical power of the reconstructed object, was found to be 17% and 20% for the RCP and LCP incident beam respectively. In our measurements we found the purity of the conversation for LCP and RCP to be ~13% and ~11% respectively. This can be further improved by using a more elaborated optimization process. The efficiency (the ratio between an optical power in the image plane and the incident power before the element) was measured to be 57%. Most of the power loss (~30%) is due to Fresnel reflection in the interface between the air and the silicon. This can be easily overcome by using an additional antireflective coating layer of silicon nitride on the back side of the fabricated element.
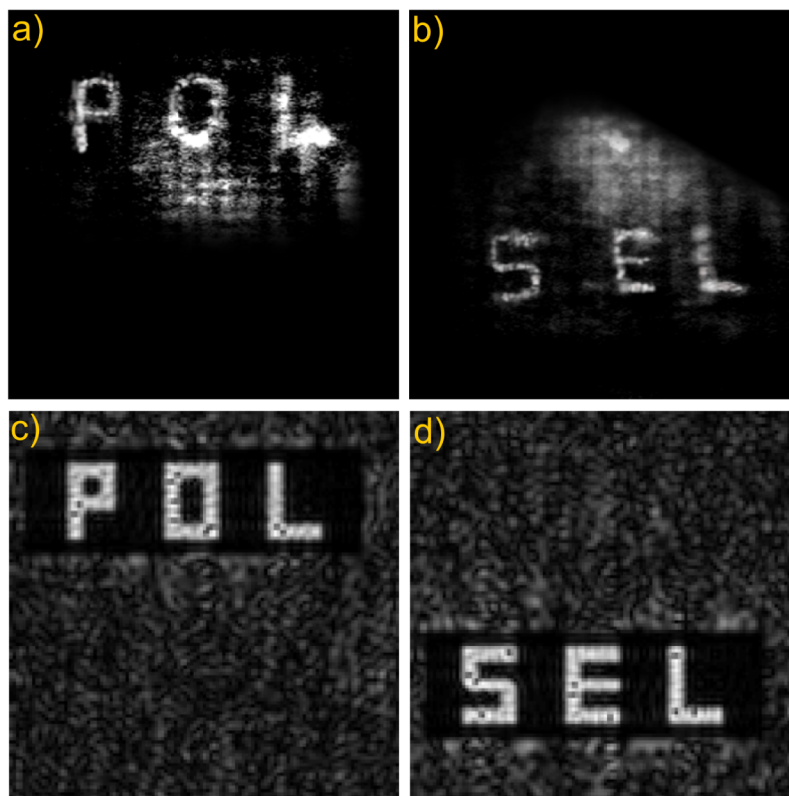

Fig. 5. Experimental result, showing the obtained images obtained by illuminating our dielectric metasurface with a) left and b) right circularly polarized light. The corresponding simulated results are shown in Fig. 5c and 5d respectively.

5. Summary

In conclusion we demonstrate the design, fabrication and experimental characterization of a dielectric metasurface acting as a polarization selective computer generated hologram, and operating at near infrared wavelength of 1550 nm. The device is based on allocating a sub wavelength grating to each pixel. By controlling the orientation of this grating one can achieve desired phase modulation. Taking advantage of the conjugate phase modulation obtained by illuminating the dielectric metasurface with LCP and RCP, we were successful in demonstrating of two independent images, for the two orthogonal polarization states. The reconstruction is obtained in the Fresnel domain. The energy in the reconstructed letters with respect to the incident power is given by the multiplication of the efficiency and the purity, i.e. it is in the range of 6%. Further improvement can be achieved by the use of AR coating

and advanced optimization. The quality of the reconstructed images can be further improved by using additional degrees of freedom, e.g. grating depth and/or duty cycle. The demonstrated concept paves the way for achieving arbitrary polarization selective beam shaping using a single dielectric metasurface.